Development and production of multi-parameter measurement device for feather pieces
Hongwei Yue, Ken Cai, Chaojun Dong, Lu Cao and Zhaofeng Zeng
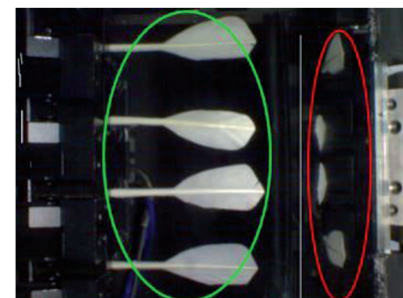
artículo ■ ■ ■ ■

Development and production of multi-parameter measurement device for feather pieces

Desarrollo y producción de un dispositivo para medición de multi-parámetros en los volantes de plumas

■ ■ ■ ■

Hongwei Yue[1], Ken Cai[2*], Chaojun Dong[1], Lu Cao[1] and Zhaofeng Zeng[3]

[1] Wuyi University, NO. 22 Dong Cheng Cun, Jiangmen, 529020, China

[2] Zhongkai University of Agriculture and Engineering, Zhongkai Road 501#, Guangzhou, 510225, Guangdong, China. kencaizhku@foxmail.com

[3] California State University, East Bay ,25800 Carlos Bee Boulevard Hayward, CA 94542, U.S.A

* Corresponding author, Ken Cai. Email: kencaizhku@foxmail.com

RESUMEN

- La correcta medición de los parámetros de las plumas es una cuestión clave para garantizar la calidad de la fabricación de volantes de bádminton. Sin embargo, la detección manual sigue siendo el principal método de medición de parámetros utilizado en la actualidad. Por eso, este estudio propone un principio de diseño y un método de medición, mediante una estructura básica con una sola cámara multi-sistema para la medición de parámetros. En primer lugar, sobre la base del principio de imagen en lente convexa, con el dispositivo de medición propuesto, se tomaron las imágenes de las plumas dentro de un espejo a diferentes ángulos. Se obtuvieron también las fórmulas para medir su curvatura, caída, ancho y espesor. En segundo lugar, se analizó la relación entre la caída y la profundidad de campo. El análisis indicó que todas la plumas con diferentes niveles de caída debían situarse dentro de los límites de la profundidad de campo para asegurar que la cámara obtenía imágenes claras. Por último, los valores medidos se compararon con los resultados obtenidos por medición manual con un calibre normal. La curvatura, caída, espesor y ancho de los trozos de pluma pueden medirse con el dispositivo propuesto de una sola cámara según los resultados prácticos obtenidos. Los resultados de este estudio pueden servir como referencia para aumentar el rendimiento y la calidad de la pluma de bádminton y reducir el coste del dispositivo y los errores humanos.

- **Palabras Clave:** imagen digital de pluma, espejo plano, curvatura y caída, medición de parámetros.

ABSTRACT

The correct measurement of feather parameters is a key issue for guaranteeing the production quality of badminton feather pieces. However, manual detection remains the main parameter measurement method used today. Therefore, this study proposed a design principle and measurement method, established the basic structure of a single-camera multi-parameter measurement system. First, on the basis of the convex lens imaging principle, images of feather pieces inside a mirror were collected at different angles with the proposed measurement acquisition device. The equations for measuring curvature, camber, width, and thickness were also derived. Second, the relationship between camber and depth of field was analyzed. The analysis indicated that the entire feather piece with different levels of camber may be set within the range of depth of field to ensure that the camera obtains clear images. Finally, the measured values were compared with the manual measurement results obtained with a vernier calibre. The curvature, camber, thickness, and width of feather pieces can be measured with the proposed single camera device according to the practical operation results. The results of this study can serve as a reference in increasing the yield and quality of badminton feather pieces and reducing device cost and subjective human errors.

Keywords: Feather digital image, planar mirror, curvature and camber, parameter measurement).

1. INTRODUCTION

The main material used to produce shuttlecocks is natural goose feather or duck feather. Sixteen pieces of feathers are required to produce one shuttlecock, and guaranteeing the flying quality of shuttlecocks requires high parameter consistency[1-3]. After purchase, raw feathers are washed, degreased (sometimes bleached), and dried in the sun (or dried using the appropriate equipment). Then, feathers of the same size and curvature are selected. After a difficult classification, every feather is cut in the appropriate section, which is then stamped. Thereafter, the actual feather pieces used for shuttlecocks are obtained. The badminton factory further classifies the feather pieces by grade and thickness before producing actual shuttlecocks. In this paper, we refer to "feather pieces" as those used to produce shuttlecocks after the stamping process. The quill root, feather quill, and feather leaf that comprise a feather piece are illustrated in Figure 1.
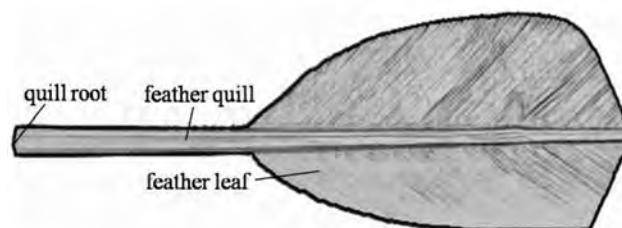

Fig. 1: Digital image of a feather piece

Feather pieces of similar parameters are important technological requirements of badminton shuttlecock production. Specifically, the curvature, camber, thickness, and width of a feather piece are the main indicators that need to be detected. The camber of a feather piece refers to the distance between the feather point

■■■ artículo

Development and production of multi-parameter measurement device for feather pieces
Hongwei Yue, Ken Cai, Chaojun Dong, Lu Cao and Zhaofeng Zeng

and the horizon when the feather piece is laid horizontally. The curvature of a feather refers to the vertical distance between the feather point and the tangent line of the quill point. The specific definitions of curvature, camber, thickness, and width are presented in Figure 2.

Current measurement methods of feather parameters mainly include artificial vision and machine vision. In artificial vision, feathers of the same parameters are obtained in an artificial manner using camber and curvature devices. This method is problematic because of factors such as high labor intensity and unstable selection quality. In machine vision, it usually adopts multiple cameras separately to detect the camber, curvature, and thickness of feather pieces[4-6]. Hence, this method entails high machine cost, numerous potential faults, and so on. Moreover, the measurement method requires segmenting the feather quill and then measuring the related camber and curvature parameters. A feather quill is usually long and thin. The feather leaf on both sides overlaps at the gray level, and the density distribution is uneven, thereby causing the gray level in the high-density area to be higher than that in the low-density area. The curvature and camber of a feather quill can aggravate uneven illumination, in which case the segmentation of a feather quill becomes impossible. Several laboratory experiments have been performed to measure and segment feather pieces[7], but measurement methods with good universality and stability have yet to be developed. To solve these problems mentioned above, a single-camera multi-parameter measurement system is further discussed in the following pages.

2. STATE-OF-THE-ART

Although machine vision technology is widely applied in many industries, the literature on the measurement of feather parameters remains limited. A homemade original feather acquisition system is presented in Figure 3[8]. Numerous experiments on feather measurement have been conducted in our laboratory, as shown in Table 1. The original device comprises three cameras and two ring-shaped LED lights. Due to considering the stability of the system, the industrial camera which has higher reliability and higher stability than the commercial camera is used. This traditional vision measurement with multiple cameras can simultaneously obtain multiple digital images of an object from different angles. However, these multiple cameras are known to suffer from several limitations: they are generally expensive, difficult to calibrate, they require exact synchronization between the cameras[9]. As a result of the multi-hardware structure of the system, ensuring the stability and real-time properties is challenging.

To overcome those problems, several works have recently proposed the use of catadioptric vision devices[10-12], which
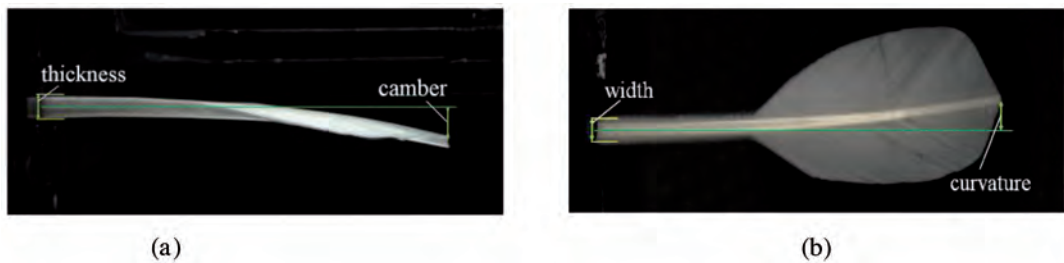

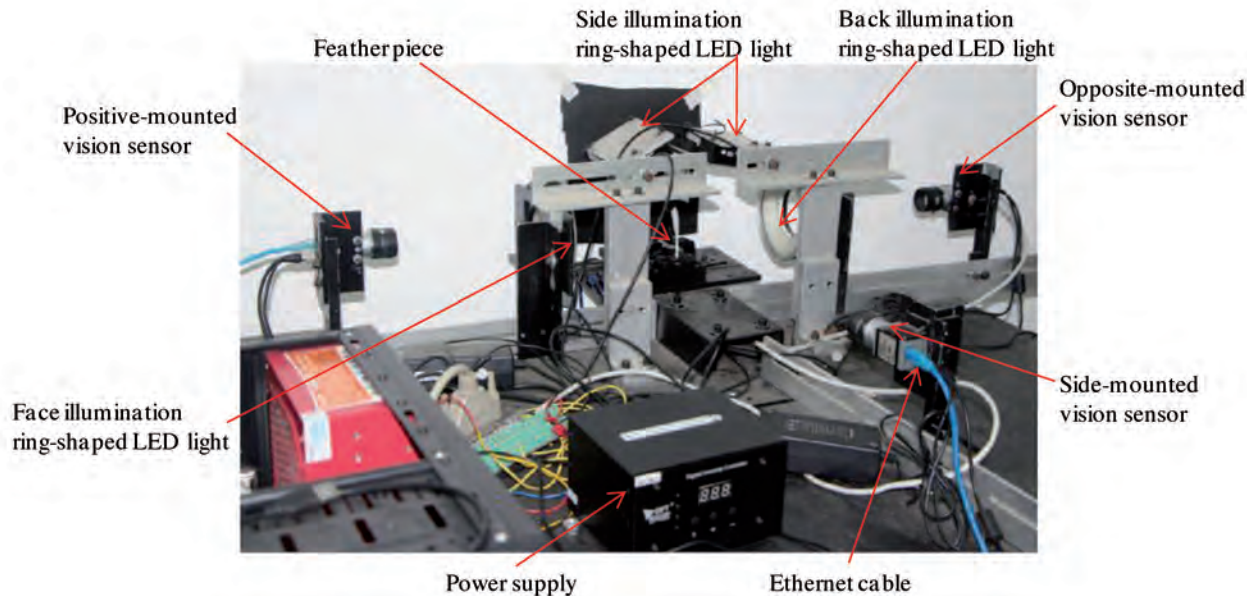Fig. 2: Parameter definition of a feather piece.(a) Camber and thickness. (b) Curvature and width

Fig. 3: Original acquisition system of feather image

Ring-shaped LED light	Camera			Purpose
Face illumination	Positive-mounted	Opposite-mounted	–	Width, area measurement
Back illumination	Positive-mounted	Opposite-mounted	–	Curvature measurement
Side illumination	–	–	Side-mounted	Camber measurement

Table 1: Composition of image acquisition system

Development and production of multi-parameter measurement device for feather pieces
Hongwei Yue, Ken Cai, Chaojun Dong, Lu Cao and Zhaofeng Zeng

artículo ▪ ▪ ▪ ▪

combine refracting(lenses) and reflecting(mirrors) elements, some authors have also introduced vision sensors composed of a single perspective camera that observes the reflections of a scene through two (or more) rigidly-attached planar mirrors[13,14]. By analyzing the literatures, these planar catadioptric vision sensors are attractive because they are equivalent to a stereo camera, they do not require any additional hardware for exact camera synchronization, and they only need a single set of internal camera calibration parameters. Here, using the idea of above study, the single-camera multi-parameter measurement system is developed and researched. To achieve an effective multi-parameter measurement of feather pieces, the present study presents a number of key technologies of the system. Two of the major issues are to construct measurement structure using planar mirror and to derive equations for parameters measurement combining convex lens imaging principle. These will be discussed in more depth in following sections.

The remainder of this paper is organized as follows. The design method of the device and the parameter measurement plan are introduced in section 3. The experimental results are presented in section 4. Finally, the main content of this research is summarized in section 5.

3. METHODOLOGY
3.1. DESIGN OF IMAGE ACQUISITION DEVICE

On the basis of the design and implementation of the Figure 3, we perform a single camera device for measuring feather piece parameters. A homemade feather acquisition device is shown in Figure 4. The experimental samples are collected from scenes of an online examination system for feather pieces. Images of the feather pieces are acquired by the CCD camera of the testing system[15-18]. Digital image acquisition is, in effect, the visual image and inherent characteristics of the object measured are converted into image data processed by a computer. The homemade detection device based on machine vision mainly includes light source, optical lens, camera, image acquisition card and etc.

The basic structure of the single camera device for measuring feather piece parameters is shown in Figure 5. This systematic device includes a computer 1, controller 2, driving power supply 3, lighting source 4, camera 5, clamp 6, feather piece 7, and planar mirror 8. The controller 2 and driving power supply 3 are both connected to computer 1. Specifically, the controller 2 controls the camera 5 to collect images. The driving power supply 3 is connected to the lighting source 4, the clamp 6 is used to hold the feather piece 7 in place, the planar mirror 8 faces toward the camera 5, and the lens center of the camera 5 shares the same horizon with the bottom level of the mirror 8[19].The camera is a MVC100SAM-GE30 CCD with resolution 1280*1024 and ethernet interface. The controller is a general KPCI-840 which has the property of high performance and
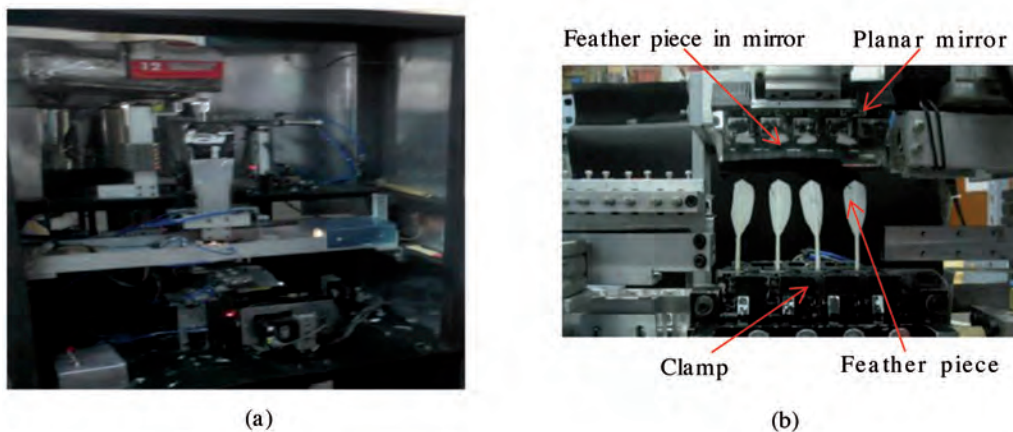

Fig. 4: Homemade feather image acquisition device.(a) Industrial feather image acquisition device in use. (b) Laboratory model
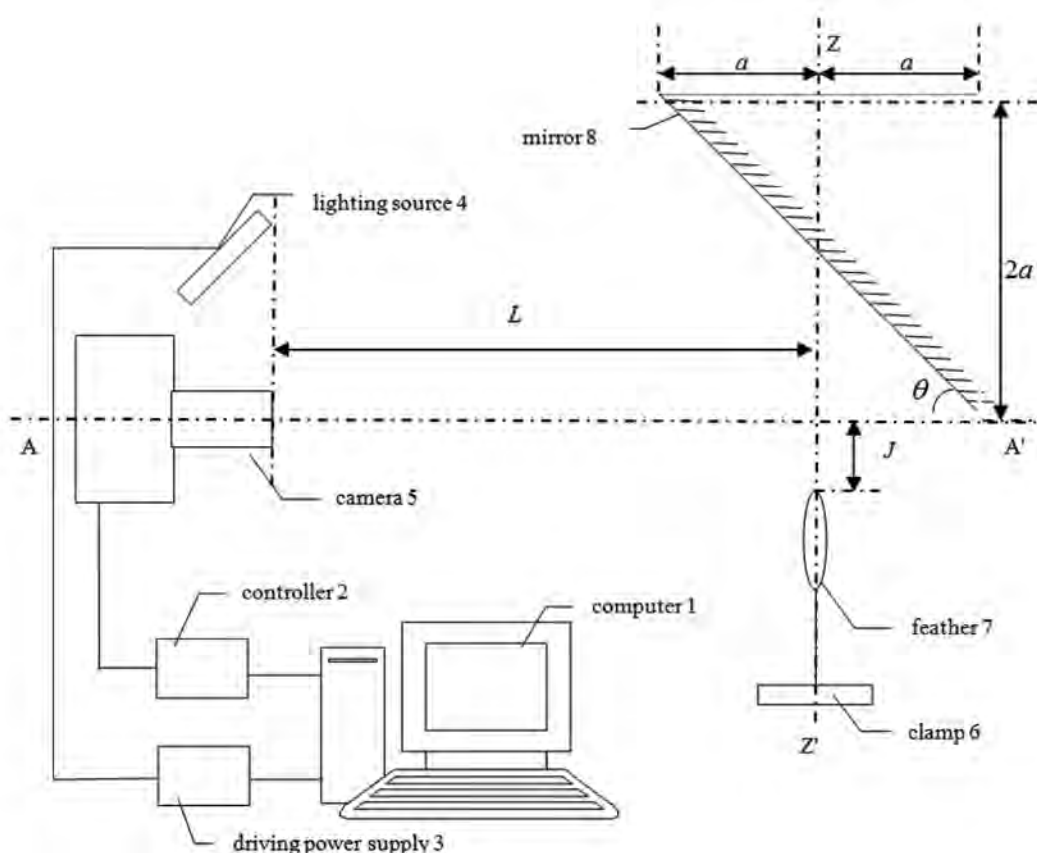

Fig. 5: Multi-parameter measurement system for feather pieces

■■■■artículo

Development and production of multi–parameter measurement device for feather pieces
Hongwei Yue, Ken Cai, Chaojun Dong, Lu Cao and Zhaofeng Zeng

friendly interface. Focal length of the lens chosen of PENTAX corporation is 8 mm.

The distance between the camera 5 and the clamp 6 is L mm, that between the feather point of the feather piece 7 and the bottom level of the mirror 8 is J mm, and the angle between the mirror 8 and the horizontal line is $\theta=45°$. The vertical distance AA' between the upper lever and the bottom level of the mirror 8 is $2a$ mm. The clamp 6 is located on the centerline ZZ ' of the mirror 8, and the lens center of the camera 5 is located on the horizontal line AA'.

3.2. PARAMETER MEASUREMENT METHODS

The images of the feather piece collected through the camera need to be analyzed. The diagram of the camber parameter measurement is shown in Figure 6. The images of the feather piece held by the clamp are shown in the ABCD area, and those inside the mirror are displayed in the CDEF area. ZZ' vertically divides the CDEF area equally, and J_1, J_2 correspond to the size of the region. p_1 represents the point position of the image of the feather piece held by the clamp, and p_2 (x_2, y_2) represents the point position of the image of the feather piece in the planar mirror.

Assume that A is the image origin. The camber of the feather piece can be calculated on the basis of the convex lens imaging principle.

1) Conduct binarization in the ABCD area of the image, and find a point p_1 of the image of the feather piece with the traversal method to determine the corresponding coordinate(x_1, y_1).

2) Use the convex lens imaging principle $L / f = J / (J_1 - x_1)$ to solve $J = L*(J_1 - x_1) / f$, where J represents the distance between the point p_1 of the real feather piece and the bottom surface of the planar mirror (shown in Fig. 5), L is the distance from the lens of

the camera to the clamp, J_1 is the distance between the two points of AD and denotes the width of the ABCD area, and x_1 is the x-coordinate of point p_1 of the feather piece. The image distance f of this system is 8 mm. The distance from the point p_1 to the line CD is the image size of J.

3) Use the relationship between object distance and image distance in the convex lens imaging principle to obtain $L*y_1=L_2*y_2$, where $L_2 = L + J + a$ represents the object distance of the feather piece point p_2 in the planar mirror. Then, $y_2=L*y_1/(L + J+ a)$ can be obtained.

4) Determine the coordinate point $p_2(x_2, y_2)$. According to y_2, determine x_2. First, conduct binarization on the images of the feather piece in the planar mirror. The binarization is performed by the maximal variance between clusters method, and then small isolated noise is eliminated through morphological algorithm. Through the binarization of CDEF area, the white area on the left and right sides of a center line ZZ' of the planar mirror can be calculated, respectively. Then, search point $p_2(x_2, y_2)$ from one side of the large area[20].

5) The distance d between $p_2(x_2, y_2)$ and the center line ZZ' can be calculated, that is $d=|J_1+J_2/2-x_2|$.

6) The camber of a feather piece is $C=(L+J+a)/f*(k*d)$, where k is the size of a pixel.

We then analyze the measurement of curvature, thickness, and width. The schematic diagram is shown in Figure 7, where the linear WW' corresponds to the clamp calibration line when the feather piece thickness is 2.5 mm and the straight line TT' corresponds to the variation position of the clamp calibration line. The calculation is as follows:

1) In the ABCD area, identify the midpoint p_3 of the quill root with the traversal method, and determine the coordinate (x_3, y_3).

Fig. 6: Schematic diagram of camber parameter measurement

2) Determine the calibration linear slope m by using a vernier caliper with an accuracy of 0.02 mm in advance. Then, determine the calibration linear slope on p_3: $y=m*x+n$.

3) Define the curvature V of the feather piece as $V = |m*x_1 + n - y_1|/\sqrt{1+m^2} *k$, where k is the size of a pixel.

4) To determine the TT' variation distance d_2 of the clamp reference line TT', define the thickness of the feather piece as $T=2.5 + (L + J + a)/f*(k*d_2)$; if WW' is located on the left of TT', then $d_2 <0$; otherwise, $d_2>0$.

5) Traverse the quill root of the feather quill to determine the width β.

3.3. ANALYSIS OF CAMBER AND DEPTH OF FIELD

The diagram of the scene imaging during the camera imaging process is shown in Figure 8(a). As shown in the figure, the size of the scenery image obtained with the
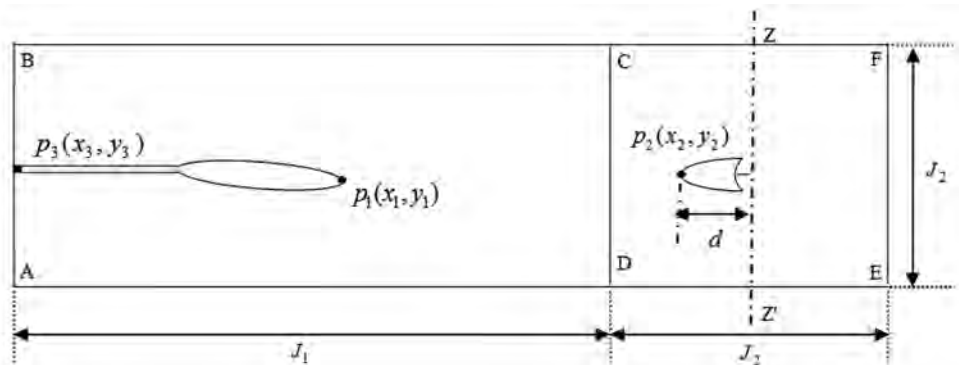

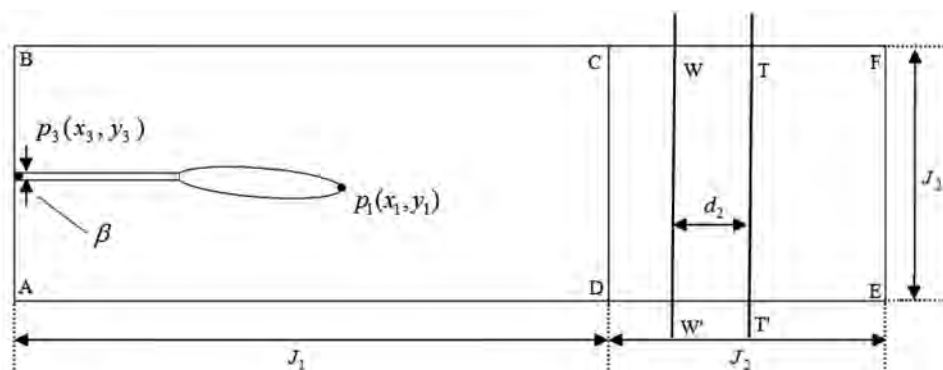*Fig. 7: Schematic diagram of curvature parameter measurement*

Development and production of multi-parameter measurement device for feather pieces
Hongwei Yue, Ken Cai, Chaojun Dong, Lu Cao and Zhaofeng Zeng

artículo ■ ■ ■ ■

photographic equipment is related to the original image size, object distance, and focal length. According to the geometrical relationship in the above figure, the size of the scenery image obtained with the photographic equipment is

$$S = \frac{f}{L} I \qquad (1)$$

Where f is the focal length, L is the object distance, S is the image size of the photographic equipment, and I is the original image size. Image size is inversely proportional to object distance; that is, a large object distance equates to a small image, and vice versa[21].

In the feather measurement process, the calibration plane is installed when the image acquisition device is installed with an industrial camera. When the measured target is located in the corresponding camera calibration plane, the camera, according to the image pixel size, can calculate the size of this target. When the measured target leaves the calibration plane, the object distance in the imaging equations changes. Thus, the camera image cannot accurately reflect the original object size. As a result of the unique shape of feathers, every piece of feather may exhibit a different camber. When a feather piece is fixed onto the image acquisition device, the feather quill remains on the calibration plane while the feather leaf parts, especially the feather point, leave the calibration plane because of the camber. In the experimental image acquisition device used in this study, the feather camber changes the object distance of the industrial camera, as shown in Figure 9.

Fig. 9: Feather deviating from the horizontal plane

As discussed previously, the curved arch shape of the feather piece causes the feather point to deviate from the calibration plane; this deviation leads to changes in object distance and errors in the final measurement data of the feather piece[22]. However, how to avoid this problem still needs to be further studied in fact. Figure 10 shows the deviation of the object distance as a result of the curved shape of the feather piece.

As a result of the different distances of the camera depth of field, feather pieces with wide camber distribution must be collected to ensure that the feather camber lies in the range of the
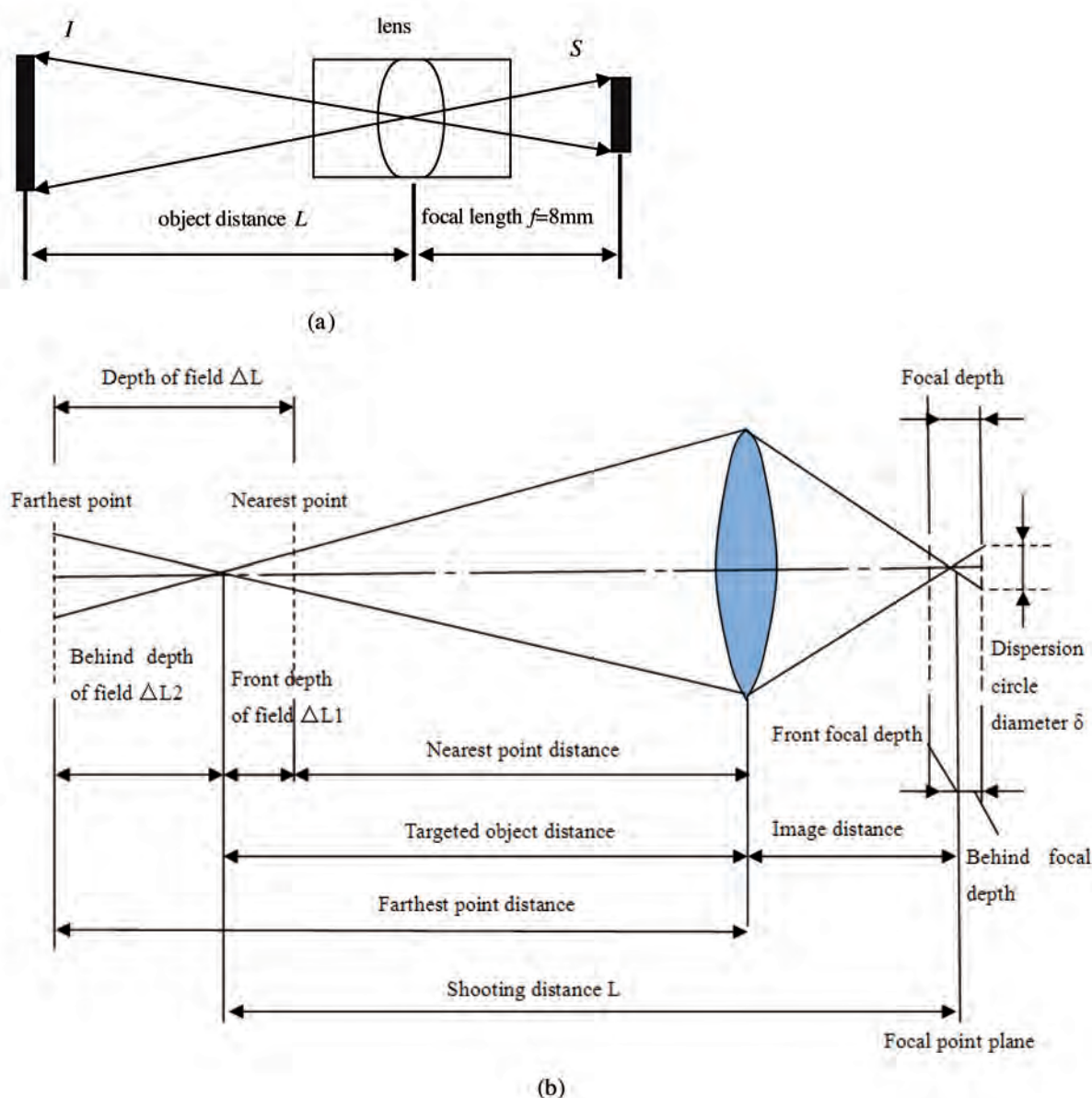

(a)

(b)

Fig. 8: Imaging scheme of convex lens. (a) Convex lens imaging principle. (b) Optical system chart of depth of field
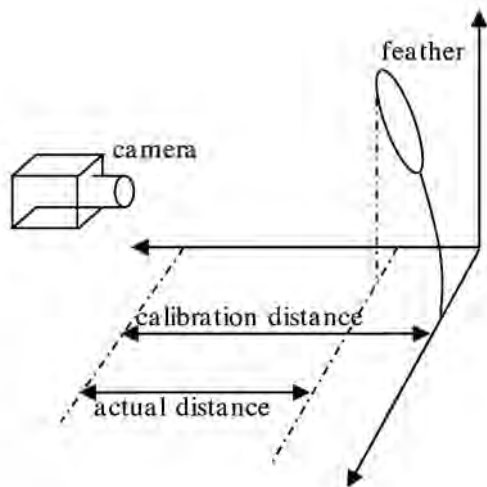
■■■■artículo

Development and production of multi-parameter measurement device for feather pieces
Hongwei Yue, Ken Cai, Chaojun Dong, Lu Cao and Zhaofeng Zeng

Fig. 10: Object distance deviation caused by feather shape

long as the dispersion circle diameter is controlled. The dispersion circle is called the permissible dispersion circle. A permissible dispersion circle is found in front of and behind the focal point, and the distance between the two dispersion circles is called the focal depth. The diagram of the depth of field formation is shown in Figure 8(b).

The depth of field ΔL includes the front depth of field and the behind depth of field, which are respectively marked as ΔL_1 and ΔL_2. The equation is as follows:

$$\Delta L_1 = \frac{F\delta L^2}{f^2 + F\delta L} \tag{2}$$

$$\Delta L_2 = \frac{F\delta L^2}{f^2 - F\delta L} \tag{3}$$

$$\Delta L = \Delta L_1 + \Delta L_2 = \frac{2f^2 F\delta L^2}{f^4 - F^2\delta^2 L^2} \tag{4}$$

camera depth of field. Then, the data can be measured and compared with the camera depth of field.

Depth of field refers to the distance between the nearest plane and the farthest plane of a clear image, which is produced by a targeted subject[23]. An ideal lens causes the light parallel to the optical axis to converge into one point. This point is called the focal point. Light gathers in front of the focal point and disperses behind the focal point. Regardless of the position in relation to the focal point, the focal point image is fuzzy and forms a circle, which is referred to as a dispersion circle. In reality, people observe images using the naked eye. However, the function of the human eye is limited. Therefore, although the original image blurs into a circle, the human eye does not perceive the image as fuzzy as

Where δ is the dispersion circle diameter, f is the lens focal length, F is the aperture value during shooting, and L is the object distance. Thus, depth of field is related to aperture value, focal length, shooting distance, permissible dispersion circle, and so on. Presume that the camera parameters are known. Then, the focal length $f=8$ *mm*, object distance $L=55$ *mm*, $F=1.4-16$, and $\delta=0.035$, as calculated in equation (4). If $F=1.4$, then $\Delta L=4.64$ *mm*; if $F=16$, then $\Delta L=68.89$ *mm*. The actual data analysis shows that the feather piece camber is mostly within 10 *mm*. As long as we appropriately adjust the aperture value, we can expect almost all feather pieces with different levels of camber to fall within the range of depth of field. This effect guarantees the clarity of camera images.
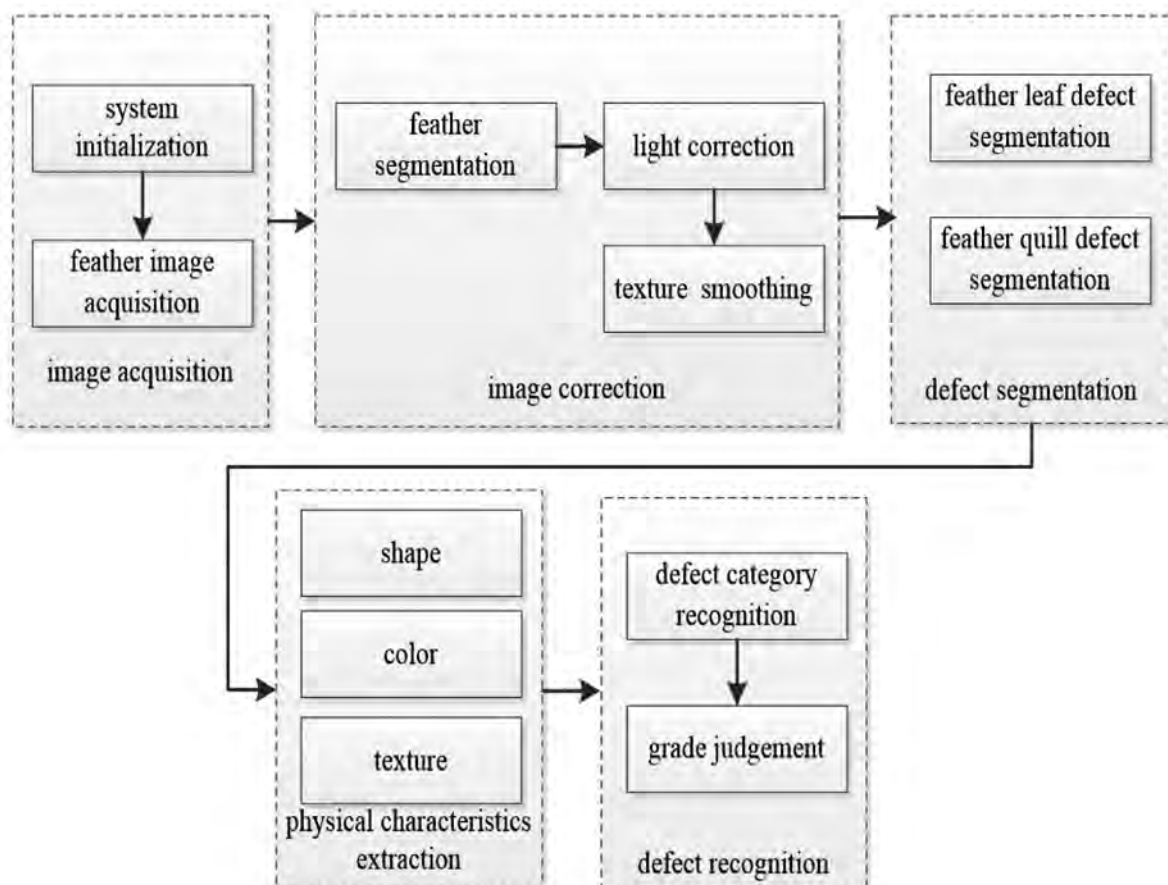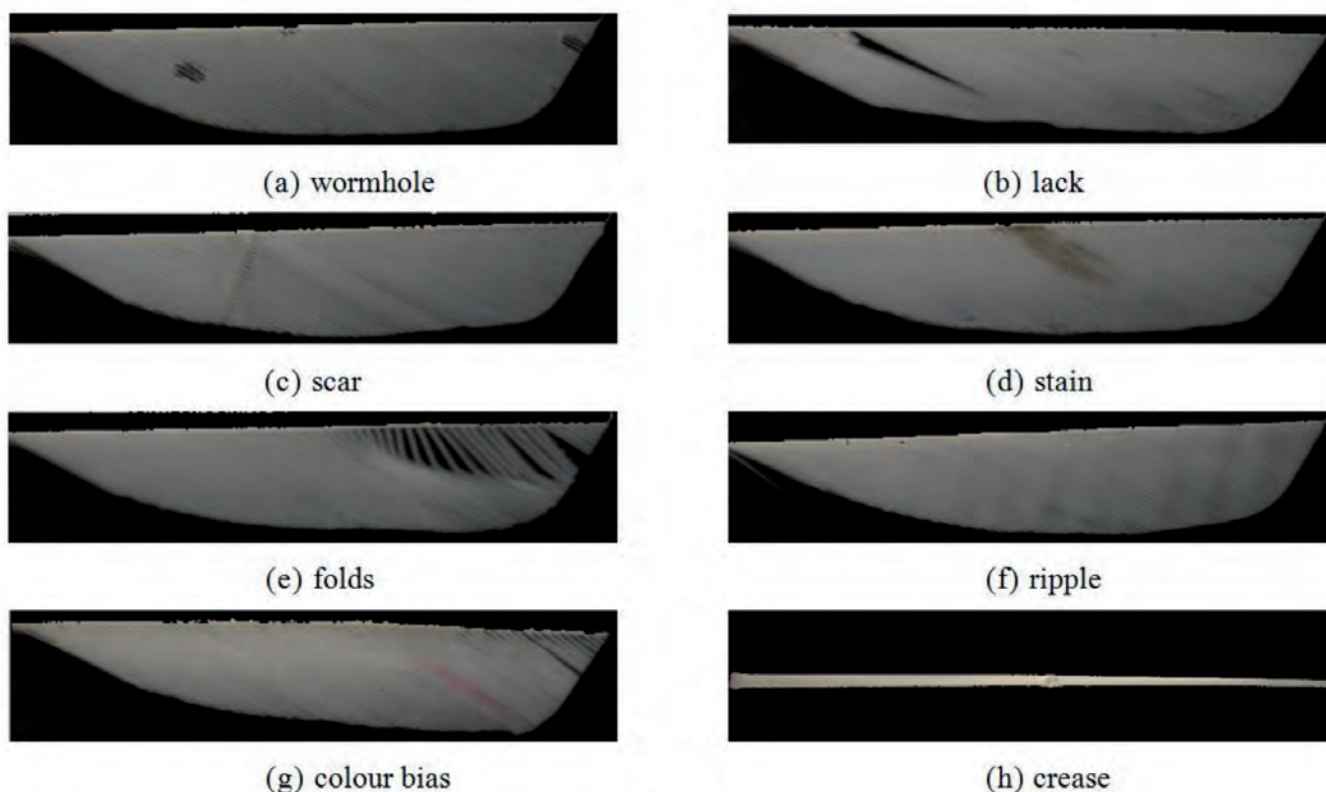

Fig. 11: Detection process of feather defect

Development and production of multi-parameter measurement device for feather pieces
Hongwei Yue, Ken Cai, Chaojun Dong, Lu Cao and Zhaofeng Zeng

artículo ■ ■ ■ ■

(a) wormhole

(b) lack

(c) scar

(d) stain

(e) folds

(f) ripple

(g) colour bias

(h) crease

Fig. 12: Eight kinds of feather defects

4. RESULT ANALYSIS AND DISCUSSION

4.1. DETECTION PROCESS OF FEATHER DEFECT

Detection process of feather piece parameters based on machine vision can be divided into the following steps, such as system initialization, feather image acquisition, light correction, texture smoothing, feather segmentation, feather quill defect segmentation, feather leaf defect segmentation, physical characteristics (shape, color and texture) extraction, defect category recognition. Detection process of a feather defect is shown in Figure 11. In the step of light correction, in order to avoid interference of external light, the entire acquisition device is placed in a sealed box; and in order to avoid as much as possible pollution of reflection light, the inside surfaces of the box is decorated with absorptivity material to reduce reflection of other objects.

The goal of the Figure 11 is to detect the presence/absence of defects in a feather image. The detected defects will be used to determine the level of a feather piece. However, accurate segmentation of defect positions, shapes, and sizes is out of the scope of this study. This paper is not about this problem.

4.2. SEGMENTATION OF FEATHER PIECES

Goose feather or duck feather may be damaged in the growth, and defiled in the process of washing, degreasing (sometimes bleaching), and drying in the sun (or using the appropriate equipment). If so, there may be many defects after processing. The defects of feather pieces mainly consists of two parts, feather leaf defect and feather quill defect, such as, wormhole, lack, scar, stain, folds, crease, ripple, colour bias, and so on dozens of defects. Figure 12 lists the eight kinds of common defects of feathers.

In order to reduce the influence of the feather quill in the subsequent processing, such as light correction, defect segmentation, etc. In this paper, One of the key things to start with is to extract feather quill to get feather leaf. So as, the follow-up steps, illumination estimation and illumination normalization, smooth filter, defect detection and identification, can easily be processed.

From the gray histogram of digital feather image (as shown in Figure 13), we can find that the gray value distribution of the feather leaf includes gray value distribution of the feather quill; thus, the traditional image segmentation methods based on image gray feature, such as edge detection algorithm based on gray discontinuity between different regions and threshold segmentation algorithm based on regional gray-scale similarity, cannot effectively extract the feather quill.It's a difficult task in segmentation of feather piece images how to extract feather quill. Therefore, this article has selected the following method. By opening the ring-shaped led light on the front, positive front-illumination image can be obtained, as shown in Figure 14(a). By opening the ring-shaped led light on the back, positive back-illumination image can be obtained, as shown in Figure 14(b).Then Figure 14(c) that results of subtracting two images of Figure 14(a) and Figure 14(b) can be obtained. Using the method of threshold binarization can get feather quill, as shown in Figure 14(d). Using feather quill can further determine whether there has crease. Then it is easy to obtain Figure 14(e). According to Figure 14(e), grade assessment
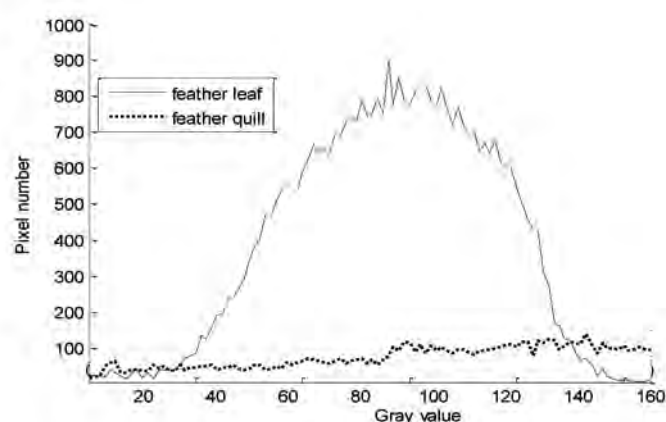

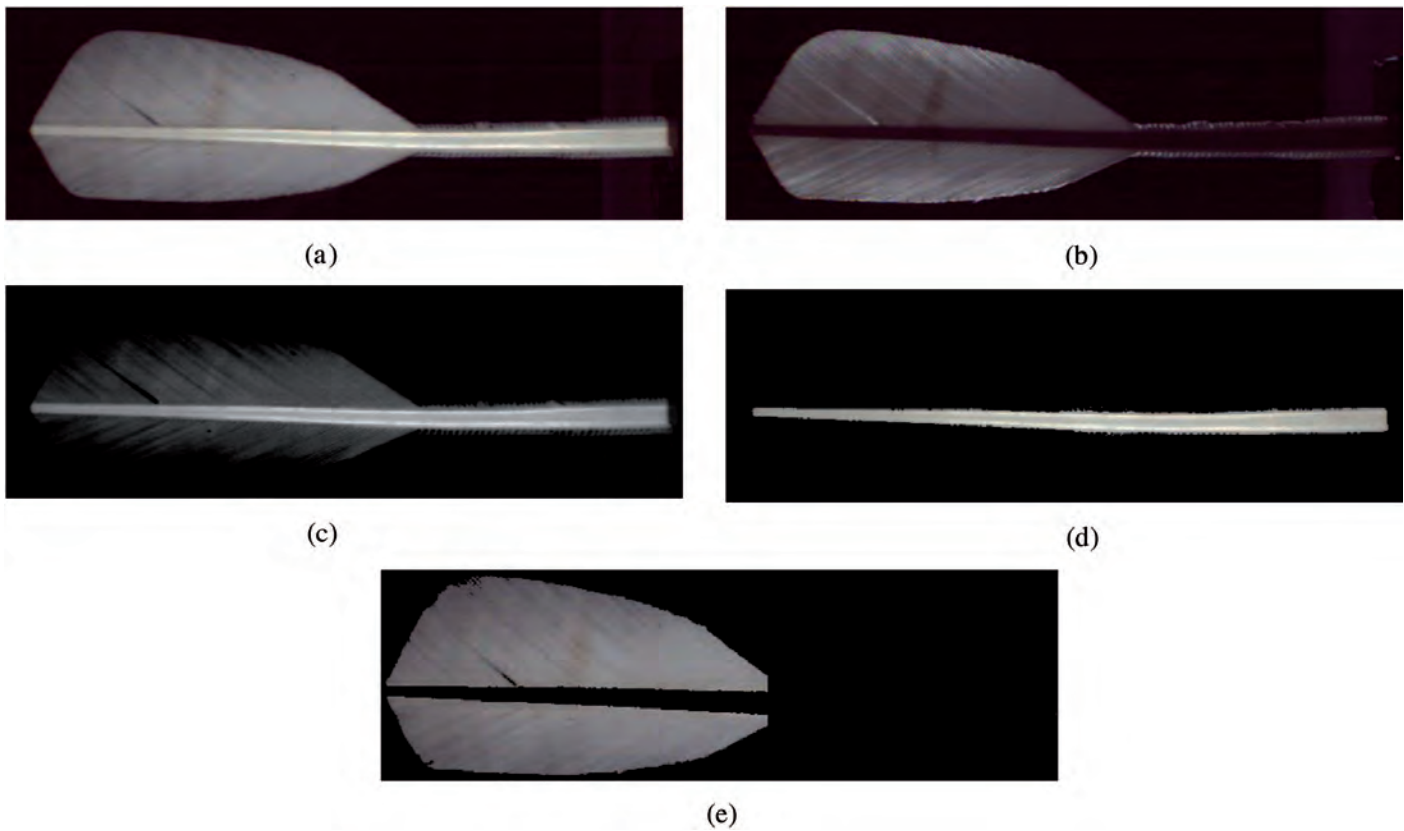*Fig. 13: Gray histogram contrast of feather leaf and feather quill*

■■■■artículo

Development and production of multi-parameter measurement device for feather pieces
Hongwei Yue, Ken Cai, Chaojun Dong, Lu Cao and Zhaofeng Zeng

Fig. 14: Segmentation of feather pieces.(a)Positive image with light on the front. (b)Positive image with light on the back. (c)Result of subtracting(b) from (a). (d) Feather quill. (e) Feather leaf

of feather leaf can further be determined through these parameters, such as shape, area, circularity and defects.

4.3. EXPERIMENTAL RESULTS OF PARAMETER MEASUREMENT

This system can handle four feather pieces simultaneously. The physical diagram is shown in Figure 15, in which the feather images inside the planar mirror are marked by a red circle and the images held by the clamp are marked by a green circle.

The upper feather shown in Figure 15 is regarded as the research object. The image of its corresponding feather piece is shown in Figure 16. Figure 17 is then obtained by conducting binarization on Figure 16[24]. By searching the binarization images, the feature points p_1, p_2, p_3 can be obtained (Figure 16). The left point corresponds to p_3(8,159), the middle point corresponds to p_1 (614,134), and the right point corresponds to p_2(969,176). Then, according to previous parameters and equations, the curvature, camber, thickness, and width can be calculated.

Fig.15: Sample of feather image
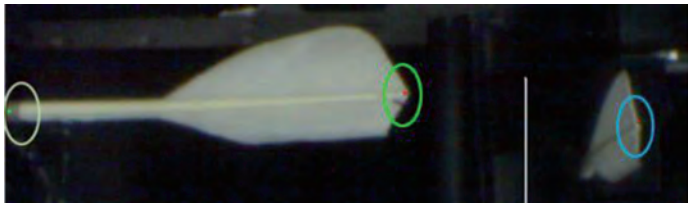
Fig.16: Calculation results of feature points

Fig.17: Binarization image of a feather piece

Table 2 and Table 3 show the feather piece parameters and compare them with artificial measurement parameters, which are obtained with a vernier caliper. In practical production, the curvature and camber of feather pieces are usually divided into eight classes: scope [0 *mm*, 1.0 *mm*) is the first class, [1.0 *mm*, 2.0 *mm*) is the second class, and so on. The thickness and width are classified as large, normal, and extra thin. For example, scope [0 *mm*, 2.0 *mm*) falls in the extra thin class, [2.0 *mm*, 4.0 *mm*) falls in the normal class, and over 4.0 *mm* falls in the large class. As shown in the tables, the width measurement error is larger than thickness measurement error. This difference is explained as follows. The thickness and width of a feather piece are measured on the
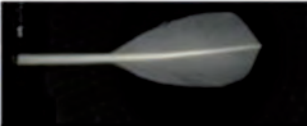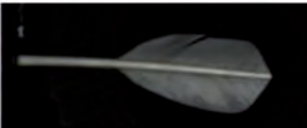
Development and production of multi-parameter measurement device for feather pieces
Hongwei Yue, Ken Cai, Chaojun Dong, Lu Cao and Zhaofeng Zeng

artículo ■ ■ ■

Sample image	Curvature (unit: mm)		Width (unit: mm)	
	Suggested method	Manual measurements	Suggested method	Manual measurements
	1.25	1.26	3.2	2.8
	−3.701*	−3.70	3.0	2.7
	3.53	3.54	2.9	2.7
	3.26	3.25	3.4	2.9
	1.61	1.60	3.4	2.9
	0.09	0.09	3.1	2.6

Table 2: Comparison of curvature and width measurement results

"−" is used to distinguish the directions of the camber and curvature

Sample image	Camber (unit: mm)		Thickness (unit: mm)	
	Suggested method	Manual measurements	Suggested method	Manual measurements
	3.31	3.32	2.6	2.6
	5.56	5.55	2.8	2.7
	−9.00	−9.01	2.6	2.5
	2.71	2.70	2.7	2.5
	−1.68	−1.69	2.7	2.7
	−8.71	−8.71	2.7	2.5

Table 3: Comparison of camber and thickness measurement results

■■■artículo

Development and production of multi-parameter measurement device for feather pieces
Hongwei Yue, Ken Cai, Chaojun Dong, Lu Cao and Zhaofeng Zeng

basis of the feather quill root. However, positioning midpoint p_3 of the feather quill root exactly is difficult because the feather quill is thin and long and features numerous thin hairs that cause significant noise during image processing. As indicated by the experimental results, the measurement parameters acquired with the device can meet the demands of feather piece classification and practical production.

5. CONCLUSION

To measure feather parameters while maintaining low machine cost and high quality, this study presented the design principle and measurement method, established the basic structure of multi-parameter measurement system. The following conclusions were obtained:

1) The device completed multi-parameter measurement, namely curvature, camber, width and thickness. Those feather parameters were the main indicators that can be detected with a single camera.

2) In this system, the planar mirror was the most important part. The angle, between planar mirror and horizontal line, was so critical to affect the above–mentioned parameter measuring method and relative calculation equations.

3) Comparing the measured values of six images with proposed method and practical operation, the measurement parameters acquired with the device can meet the demands of feather piece classification and practical production. Besides, the device can process four feather images simultaneously.

4) The multi-parameter measurement system with one camera has the characteristic of low cost in comparison with the original device with three cameras.

With this device, labor intensity can be greatly reduced, and production efficiency is significantly improved. The results lay a solid foundation for badminton production automation in the future. Our future study will focus on a measurement method that could address issues such as stains of feathers, damage caused by worms, and color deviation.

BIBLIOGRAPHY

[1] Alam F, Chowdhury H, Theppadungporn C, et al. "Measurements of aerodynamic properties of badminton shuttlecocks". *Procedia Engineering*. June 2010. Vol. 2-2. p. 2487-2492. DOI: http://doi.org/10.1016/j.proeng.2010.04.020

[2] Lin CSH, Chua CK, Yeo JH. "Turnover stability of shuttlecocks-transient angular response and impact deformation of feather and synthetic shuttlecocks". *Procedia Engineering*. September 2013. Vol. 60. p. 106-111. DOI: http://doi.org/10.1016/j.proeng.2013.07.024

[3] Lin CSH, Chua CK, Yeo JH. "Aerodynamics of badminton shuttlecock: Characterization of flow around a conical skirt with gaps, behind a hemispherical dome". *Journal of Wind Engineering and Industrial Aerodynamics*. April 2014. Vol. 127. p. 29-39. DOI: http://doi.org/10.1016/j.jweia.2014.02.002

[4] Wang Y, Yan XF, Zhang W."An Algorithm of Feather and Down Target Detection and Tracking Method Based on Sparse Representation". *IEEE 7th International Conference on Measuring Technology and Mechatronics Automation (ICMTMA)*.June 2015. Vol. 2015. p.87-90. DOI: http://doi.org/10.1109/ICMTMA.2015.28

[5] Yan XF, Wang YQ. "Research on Application of Sparse Representation in Feather and down Category Recognition". *Proceedings of the 4th International Conference on Intelligent System and Applied Material*. August 2014. Vol. 1049. p.1297-1301. DOI: http://doi.org/10.4028/www.scientific.net/AMR.1049-1050.1297

[6] Liu HJ, Wang R, Li XC. "Improved algorithm of feather image segmentation based on active contour model". *Journal of Computer Applications*. August 2011. Vol. 32-8. p. 2246-2245

[7] Yue HW, Wang RH, He ZH. "Automatic extraction of feather quill based on Normalized cut algorithm". *Journal of Computer Applications*. July 2012. Vol. 32-7. p. 1899-1901

[8] YUE H, CAI K, LUO B, et al. "Denoising and Segmentation of Digital Feather Image Using Mean Shift Algorithm". *Journal of Digital Information Management*. February 2015. Vol. 13-1. p. 25-30

[9] Yang R, Guan P, Cai K, et al. "A novel approach to synchronous image acquisition from near infrared camera in optical-surgery navigation system". *Journal of Engineering Science and Technology Review*. October 2015. Vol. 8-3. p. 14-20

[10] Svoboda T, Pajdla T. "Epipolar geometry for central catadioptric cameras". *International Journal of Computer Vision*. August 2002. Vol. 49-1. p. 23-37. DOI: http://doi.org/10.1023/A:1019869530073

[11] Wu HHP, Lee MT, Weng PK, et al. "Epipolar geometry of catadioptric stereo systems with planar mirrors". *Image and Vision Computing*. July 2009. Vol. 27-8. p. 1047-1061. DOI: http://doi.org/10.1016/j.imavis.2008.09.007

[12] Gluckman J, Nayar SK. "Catadioptric stereo using planar mirrors". *International Journal of Computer Vision*. August 2001. Vol. 44-1. p. 65-79. DOI: http://doi.org/10.1023/A:1011172403203

[13] Wu HHP, Chang SH. "Fundamental matrix of planar catadioptric stereo systems". *IET Computer Vision*. June 2010. Vol.4-2. p. 85-104. DOI: http://doi.org/10.1049/iet-cvi.2008.0021

[14] Mariottini GL, Scheggi S, Morbidi F, et al. "Planar mirrors for image-based robot localization and 3-D reconstruction". *Mechatronics*. June 2012. Vol.22-4. p. 398-409. DOI: http://doi.org/10.1016/j.mechatronics.2011.09.004

[15] Burke MW. *Image Acquisition: Handbook of Machine Vision Engineering (Vol.1)*. First edition. Springer, 2012. p.65-123. ISBN: 9-40-090069-4

[16] Figliola RS, Beasley D. *Theory and design for mechanical measurements*. First edition. John Wiley & Sons, 2015. p.2-31. ISBN: 1-11-888127-3

[17] Seyid K, Popovic V, Cogal O, et al. "A real-time multiaperture omnidirectional visual sensor based on an interconnected network of smart cameras". *IEEE Transactions on Circuits and Systems for Video Technology*. February 2015. Vol. 25-2. p. 314-324. DOI: http://doi.org/10.1109/TCSVT.2014.2355713

[18] Mariottini GL, Scheggi S, Morbidi F, et al. "Planar mirrors for image-based robot localization and 3-D reconstruction". *Mechatronics*. June 2012. Vol. 22-4. p. 398-409. DOI: http://doi.org/10.1016/j.mechatronics.2011.09.004

[19] Tokunaga M, Egi H, Hattori M, et al. "Improving performance under mirror-image conditions during laparoscopic surgery using the Broadview camera system". *Asian journal of endoscopic surgery*. January 2014. Vol.7-1. p. 17-24. DOI: http://doi.org/10.1111/ases.12080

[20] Xu L, Feng Y, Fan Z, et al. "Research into the grading method of kiwi fruit based on volume estimation and surface defect". *INMATEH-Agricultural Engineering*. September 2014. Vol.44-3. p. 93-102

[21] Feng D, Feng MQ, Ozer E, et al. "A vision-based sensor for noncontact structural displacement measurement". *Sensors*. July 2015. Vol.15-7. p. 16557-16575. DOI: http://doi.org/10.3390/s150716557

[22] Zhan D, Yu L, Xiao J, et al. "Multi-Camera and Structured-Light Vision System (MSVS) for Dynamic High-Accuracy 3D Measurements of Railway Tunnels". *Sensors*. April 2015. Vol.15-4. p. 8664-8684. DOI: http://doi.org/10.3390/s150408664

[23] Han F, Duan J, Wang K. "Study and model construction for camera depth of field in machine vision inspection system". *Journal of sensing technology*. December 2010. Vol. 23-12. p. 1744-1747. DOI: http://doi.org/10.3969/j.issn.1004-1699.2010.12.015

[24] Klancnik S, Ficko M, Balic J, et al. "Computer vision-based approach to end mill tool monitoring". *International Journal of Simulation Modelling*. October 2015. Vol. 14-4. p. 571-583. DOI: http://doi.org/10.2507/IJSIMM14(4)1.301